9-25-2024

Modeling of Carbon Black Formation During Methane Pyrolysis

Matthew Veselinovic
University of Windsor

Modeling of Carbon Black Formation During Methane Pyrolysis

By

Matthew Veselinovic

A Thesis

Submitted to the Faculty of Graduate Studies
through the Department of Mechanical, Automotive and Materials Engineering
in Partial Fulfillment of the Requirements for
the Degree of Master of Applied Science
at the University of Windsor

Windsor, Ontario, Canada

2024

Modeling of Carbon Black Formation During Methane Pyrolysis

by

Matthew Veselinovic

APPROVED BY:

_____

I. Xu
Department of Civil and Environmental Engineering

_____

R. Balachandar
Department of Mechanical, Automotive and Materials Engineering

_____

N. Eaves, Advisor
Department of Mechanical, Automotive and Materials Engineering

September 3, 2024

DECLARATION OF ORIGINALITY

I hereby certify that I am the sole author of this thesis and that no part of this thesis has been published or submitted for publication.

I certify that, to the best of my knowledge, my thesis does not infringe upon anyone's copyright nor violate any proprietary rights and that any ideas, techniques, quotations, or any other material from the work of other people included in my thesis, published or otherwise, are fully acknowledged in accordance with the standard referencing practices. Furthermore, to the extent that I have included copyrighted material that surpasses the bounds of fair dealing within the meaning of the Canada Copyright Act, I certify that I have obtained a written permission from the copyright owner(s) to include such material(s) in my thesis and have included copies of such copyright clearances to my appendix.

I declare that this is a true copy of my thesis, including any final revisions, as approved by my thesis committee and the Graduate Studies office, and that this thesis has not been submitted for a higher degree to any other University or Institution.

ABSTRACT

Decarbonization of the energy generation sector is a very important step to attaining a Net-Zero Carbon economy. Countries, including Canada, have begun phasing out the use of fossil fuels and direct burning of natural gases as energy sources. However, Canada has rich natural gas resources primarily composed of methane that must find a viable use with the direct combustion of methane and other fossil fuels being phased out. One of these uses include methane pyrolysis, the synthesis of "turquoise" low-carbon hydrogen with the co-generation of Carbon Black, or soot, as an added economic incentive. Popular pyrolysis methods such as steam methane reforming, are very expensive and emission intensive. A novel development made by Ekona Power Inc. has found a cleaner use for Canada's rich methane resources. This research paper is to develop affordable chemical kinetics mechanisms that are able to create accurate predictions for both the physical soot as well as the hydrogen production through the methane pyrolysis process and to understand qualitative trends in pyrolysis modeling. Currently, there are many literature mechanisms available for particle simulation, however, there has been no systematic testing of these mechanisms for methane pyrolysis. Understanding when to best utilize each mechanism given specific temperature and pressure ranges will hopefully decrease computational costs and time.

ACKNOWLEDGEMENTS

First, I would like to express my gratitude to my supervising professor Dr. Nickolas Eaves for his guidance, motivation and support throughout the entire process of my journey in acquiring my Master degree. His dedication to bringing out the best in his research students has led us to strive for excellence in our work.

I would also like to give my thanks to my research partners at Ekona Power Incorporated, specifically Donald Kendrick, Mehran Dadsetan, and Scott Gray for their guidance during the completion of my research.

I also thank my Master committee of Dr. Ram Balachandar and Dr. Iris Xu for their crucial input in the completion of my thesis. I extend my gratitude to my research colleagues in the NanoACE group for creating a positive working environment throughout my entire Master journey.

Finally, I would like to thank my family and friends for their love and support. Without them this thesis and my journey through my Master degree would not have been possible.

TABLE OF CONTENTS

LIST OF TABLES

LIST OF FIGURES

CHAPTER 1

INTRODUCTION

1.1 Motivation

Humanity has always had a desire for innovation. As civilization has developed throughout history, from the industrial revolution to modern society, the demand for energy has always been a top priority. There have been many different ways in which this electrical power has been generated, from the earliest coal-steam generators of the 19th century to the burning of natural gases in the 21st century. While there have been other methods present that produce cleaner energy such as hydroelectricity, solar power and wind energy, the demand for power during the 20th century was too vast and these means of clean energy proved to be too inefficient and expensive. Due to how relatively cheap the burning of coal and other fossil fuels, such as oil and natural gas, were as a power source, it became incredibly widespread. The main issue with burning these fossil fuels is that it releases Greenhouse Gases (GHG) and Carbon Dioxide (CO2) into the atmosphere. In fact, the burning of these fossil fuels is the leading cause of global climate change accounting for roughly 75% of GHG and nearly 90% of all CO2 emitted [1]. The release of these gases into the atmosphere leads to what is known as the greenhouse effect. This is when gases released into the atmosphere do not allow heat to escape, thus increasing the temperature of the planet [2]. While the energy generation sector is not the sole contributor of GHG and CO2 released, it is a large contributor with the energy sector representing a quarter of GHG emitted in the United States in 2022 [3].

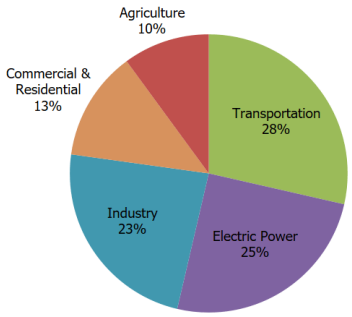

Figure 1: US GHG Emissions Per Sector 2022 [3]

Due to research completed studying the effects of CO2 and other GHG in their contribution to climate change, many governments have begun phasing out the direct burning of fossil fuels as an energy source. This will unfortunately take lots of time to fully set into motion, as large economic incentives are pushing against the shift in paradigm necessary to have a Net-Zero Carbon Emission society. This can be seen as international and national programs to reduce emissions have been put into place such as the Paris Agreement and the Powering Past Coal Alliance [4]. While many countries have joined these initiatives to reduce their emissions, globally we have only seen growth in power generation-related emissions from 33.1 gigatons of CO2 released in 2018 [5] to 36.8 gigatons of CO2 released in 2022 [3].

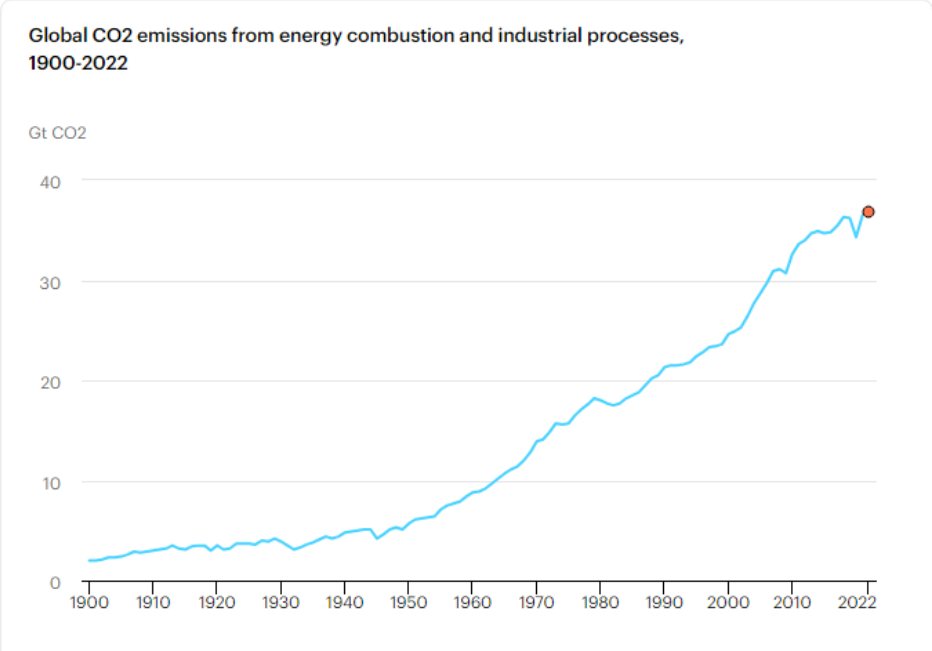

Figure 2: Global CO2 Emissions from Energy Combustion and Industrial Process 1900-2022 [7]

Canada, a world leader in its fight against climate change, being one of the founding members of the Powering Past Coal Alliance, has fortunately seen a decrease in its GHG emissions. This is due to the fact that the Canadian power generation sector has begun phasing out the use of fossil

fuels and direct burning of natural gases, such as methane, as energy sources. With GHG emitted by the Canadian power generation sector decreasing by 2% from 2018 to 2019 and decreasing by a further 9% from 2019 to 2020 [8], innovative clean energy producing methods are in the forefront of the Canadian power industry. Initiatives such as the Hydrogen Strategy [9], have been put in place to ensure that Canada utilizes its resources in new and meaningful ways. Since the direct burning of natural gases such as methane produce lots of CO2, this process has begun slowly phasing out of the power generation industry. However, there are still vast reserves of methane found underground in parts of western Canada. This leads to the question of what this methane can be used for now that its direct burning is no longer being considered.

1.2 Scope of Work

This research is intended to utilize chemical mechanisms present in established literature and rigorously test them with a novel pyrolysis method to have a better understanding of when each of the mechanisms perform in a best-case or worst-case scenario depending on various inputs. A best-case scenario is defined by a mechanism simulating particle formation or decomposition at a faster rate when compared with the other chemical mechanisms. A worst-case scenario is defined as when a chemical mechanism predicts yields forming or decomposing at a slower rate compared with the other chemical mechanisms. Since each of the mechanisms differ from each other, we want to understand the qualitative differences in their simulations. There is still a level of uncertainty that must be taken into account in this study as the comparisons between mechanisms are qualitative in nature. However, by gaining a better understanding of how the literature mechanisms behave in a pyrolysis setting and understanding the trends in the results, we can then know when to utilize each mechanism to save computational time and energy for future pyrolysis

simulations. This is achieved by lowering the number of chemical mechanisms needed to be run to attain complete coverage of key species formation or decomposition in the pyrolysis reaction.

1.3 Outline of Thesis

The thesis is divided into 4 Chapters. Chapter 2 will delve into the Background of the research, giving a review of past and present methods of hydrogen production and methane pyrolysis. Chapter 3 is about the Chemical Mechanisms that are utilized in the study, including an explanation of what each of the literature mechanisms are, how they are run and how they were changed for the pyrolysis process. Chapter 4 goes into the Results of the simulation work, giving an explanation of the outcome and the impact of better understanding the literature mechanisms. Chapter 5 concludes the paper as well as gives a direction of where future work could be headed in this field of research.

CHAPTER 2

BACKGROUND

2.1 Importance of Hydrogen

Canada still has large reserves of natural gas, such as methane, that need to be utilized. In the past, natural gas was burned directly as a fuel source. Due to the composition of methane (CH4) and other natural gases, when they are mixed with oxygen and burned, they release harmful GHG such as CO2 into the atmosphere. Since the goal of countries shifting from the direct burning of coal as an energy source is to lower their emissions, it was counter-intuitive that the replacement energy source also releases lots of CO2. To counteract this, new and innovative ways of utilizing natural gas must be found.

Looking at the chemical composition of methane, hydrogen is present. Hydrogen is a very important gas for a carbon-free future. This is due to the fact that hydrogen can also be directly burned as a fuel source. The key difference in burning hydrogen as compared to burning methane and other natural gases is that it releases no CO2 or other GHG, and it produces water. There are currently many different uses for hydrogen in energy production such as in rocket fuel, fuel cells in automotive or aeronautical vehicles, and electricity generation for homes and industry. With an ever-changing and innovating society pushing for environmentally friendly energy sources, it is possible that hydrogen will be used in many more power and electricity generation settings in the future.

2.2 Hydrogen Generation

Due to the importance of hydrogen in a carbon-free future, many different methods of generating it have been introduced and tested in the energy generation sector. The current most popular form

of hydrogen generation is Steam-Methane Reforming (SMR). This is the process in which heated steam and a catalyst are mixed with methane which causes the methane to break down into carbon monoxide (CO) and hydrogen gas (H2). The carbon monoxide will then mix further with the steam causing more hydrogen gas to form, but unfortunately also releasing CO2.

Process	Reaction Equation
Steam reforming (SR)	(1) $CH_4+H_2O \rightarrow CO+3H_2$ (2) $CO+H_2O \rightarrow CO_2+H_2$

Figure 3: The Steam Methane Reforming Process [10]

Steam methane reforming utilized in the energy generation sector does not generate clean hydrogen, it produces what is known as Grey Hydrogen. Since the hydrogen being generated is supposed to burn as a clean carbon-free energy source and the process of SMR releases CO2 into the atmosphere, the process is not a viable replacement for current energy sources. SMR is currently the most popular hydrogen generation method because it is the most economically viable.

Another form of hydrogen generation that is present is electrolysis. Electrolysis is the process in which water is separated into hydrogen gas and oxygen gas. Using electricity in either a fuel cell or an electrolyser, charges are passed through two electrodes causing hydrogen to form at the negatively charged cathode and oxygen to form at the positively charged anode [11]. This process generates what is known as Green Hydrogen since there is no CO2 being released during the formation process. The main issue with electrolysis is that it is very energy intensive, and similar to SMR, it utilizes lots of water in its hydrogen generation process.

In an effort to combat these issues with the current forms of hydrogen generation, a new form of hydrogen production was theorized. The hydrogen that would be created in this tier would be more

financially viable than Green Hydrogen and would produce little to no CO2 as compared to Grey Hydrogen. This new division of produced hydrogen was called Turquoise Hydrogen.

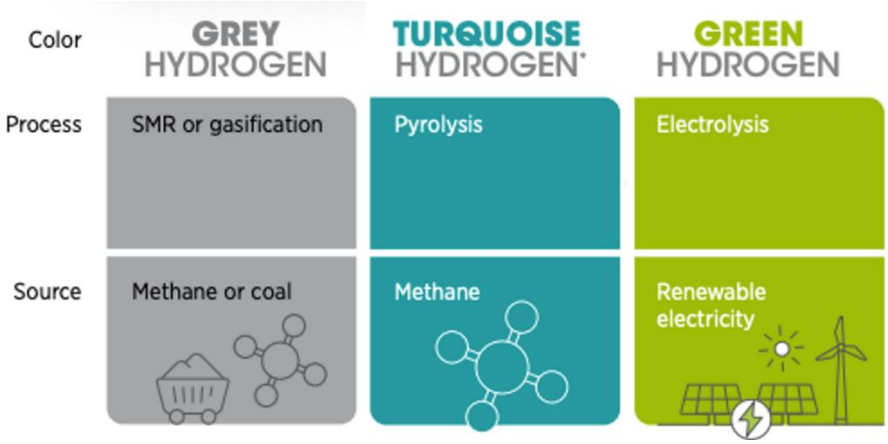

Figure 4: Differing Tiers of Hydrogen Production [12]

The main process that is highlighted in the formation of Turquoise Hydrogen is methane pyrolysis. A newly emerging decarbonization method, methane pyrolysis is the process of directly splitting, or cracking, methane into its most basic components. This is done by heating methane in the absence of oxygen, and thus does not release any CO2 as a biproduct. The only direct products of the pyrolysis process are carbon in a solid form, which can be referred to as soot or carbon black, and hydrogen gas. As previously stated, the produced hydrogen can be utilized for various energy generation methods, while the produced carbon black can be sold as an added economic incentive to the methane pyrolysis process, specifically in the plastics and tire manufacturing industries.

Methane pyrolysis is considered to generate Turquoise Hydrogen since it produces very little to no CO2 as compared with SMR and other producers of Grey Hydrogen, and it is more economically feasible than electrolysis and other producers of Green Hydrogen. This can be seen as the as the enthalpy required for the electrolysis process ($286 \frac{kJ}{mol_{H_2}}$) is several times larger than that of the enthalpy required for the pyrolysis process ($37.5 \frac{kJ}{mol_{H_2}}$) [13].

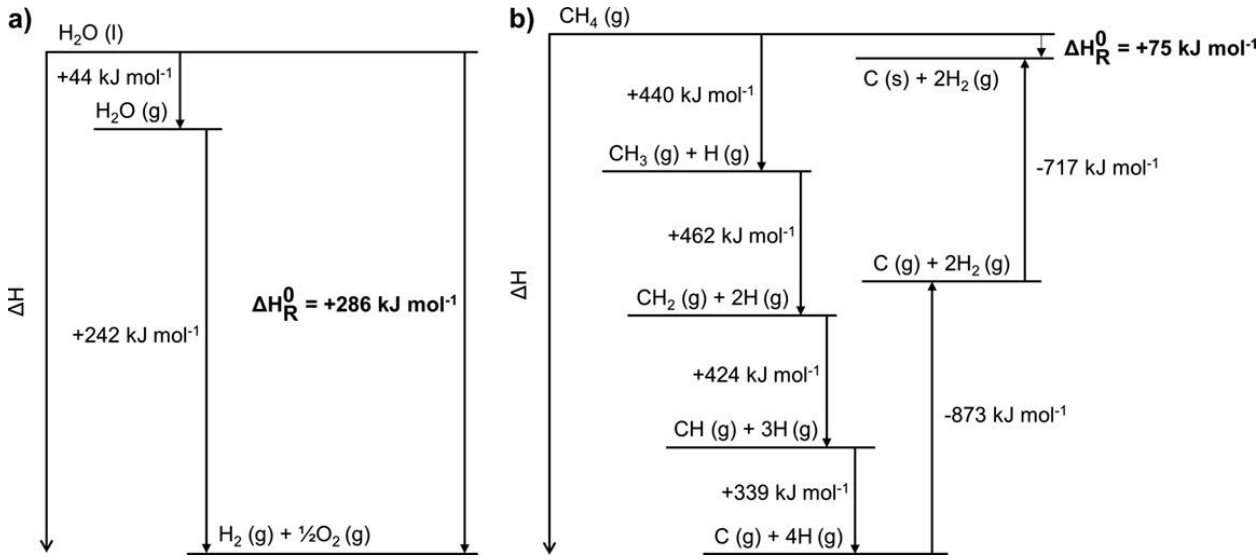

Figure 5: Enthalpy Diagram for Electrolysis and Methane Pyrolysis [13]

Pyrolyzing methane has been theorized and tested to be achieved in several ways, and the most common methods are through the use of a catalyst, through the use of plasma or by a thermal process. Pyrolysis is a high temperature endothermic reaction where the decomposition of the hydrogen-carbon bonds generally occurs above 1000°C (1273K). In most settings, maintaining an environment with temperatures this high is extremely energy intensive, which is why a catalyst can be utilized. The purpose of a catalyst is to lower the reaction temperature necessary for the pyrolysis process to occur. There have been many solid metal and carbon catalysts that have been tested on the pyrolysis process with success, however, the main issue with the utilization of a catalyst in a pyrolysis reaction is catalytic deactivation [14]. This deactivation is generally caused by poisoning or clogging of active sites on the catalyst [15]. When deactivation of a catalyst occurs, product quantity and quality as well as rate of reaction will all decrease. Therefore, until a method of reactivation of catalysts is discovered, the utilization of catalysts in pyrolysis reactions are not ideal for mass commercialization.

Another form of methane pyrolysis involves the use of a plasma reactor. Plasma, generally regarded as being the fourth state of matter, is when gas enters a super-heated state to the point in

which the electrons are stripped from the atoms of the gas, thus creating an ionized gas [16]. There are many different plasma reactors that can be used in the methane pyrolysis process; however, the most common form is Dielectric Barrier Discharge (DBD) plasma reactors [17]. These small cylindrical reactors utilize the highly energetic electrons present in the ionized gas to directly impact the methane molecules, thus causing the separation into hydrogen and carbon. These reactors are unfortunately not efficient as their conversion rate of methane into hydrogen and carbon generally does not exceed 50% [17]. Therefore, until a way to ensure a higher conversion factor for these reactors is achieved, large scale methane pyrolysis through the utilization of a plasma reactor is not financially viable.

The third common form of methane pyrolysis is achieved solely through a thermal generation process. These are generally harder to achieve and maintain since the reaction temperature for pyrolysis to occur is so high. One common method to achieve these temperatures is through heating the pyrolysis chamber walls to a desired temperature. While this does work, it is inefficient because even though some of the methane present on the chamber walls will pyrolyze into carbon and hydrogen gas, there is still a large amount of methane in the center of the chamber that will not be heated to the proper temperature for decomposition. A way to possibly combat this is to have a mixer present that will move the heated gases present along the chamber walls and disperse it throughout the rest of the chamber. Unfortunately, due to the second law of thermodynamics, there will be a large temperature drop once the heated gases are mixed with the non-heated central gases. To combat this, the size of the chamber must be drastically reduced in order for the temperature loss to be reduced, or the temperature of the chamber walls must be increased by a significant amount. This is so that when the temperature does drop, the methane will still have the necessary thermal energy to undergo the pyrolysis process. Currently, neither of these solutions would make

the thermal pyrolysis process through chamber wall heating economically viable because the chamber will either be too small or too expensive to maintain at the elevated temperature required for complete pyrolysis.

2.3 Pulsed Methane Pyrolysis

While very few of the solely thermal processes are financially viable for pyrolysis at a large scale, a power generation start-up company located in British Colombia, Canada; Ekona Power Incorporated, has theorized a possible solution. Rather than heating the pyrolysis chamber through the walls of the chamber, Ekona utilizes a pre-pyrolysis chamber combustor as can be seen below in Figure 6.

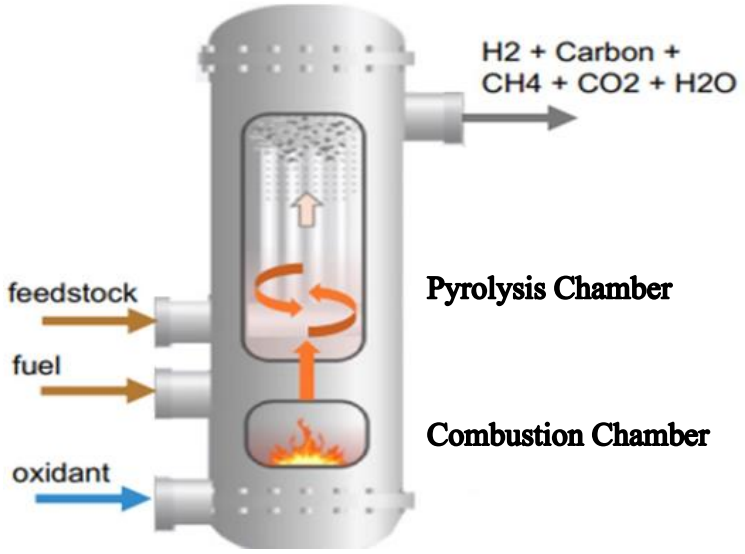

Figure 6: Ekona's Pyrolysis Chamber and Combustor

This combustion chamber generates the heat that is required for the pyrolysis process to occur in the pyrolysis chamber. The fuel and an oxidant are mixed into the combustion chamber where the combustion reaction then occurs. In a pulsed manner, some of the heated gas from the combustion process is fed into the pyrolysis chamber where some of the feedstock of methane is simultaneously released. The mixing of these two pulsed gases then allows for the pyrolysis of the

methane to take place. Rather than having all of the energy spent on generating the heat necessary for the pyrolysis process to occur dissipate into a large chamber of lower temperature gas, an isolated amount of both the combusted gases and the feedstock are mixed together and pyrolyzed. This lowers the energy cost compared to other thermal pyrolysis processes as the energy waste is much lower. One drawback to Ekona's Pulsed Methane Pyrolysis (PMP) process compared with other pyrolysis processes is that it releases CO2. With an oxidant necessary in the combustion chamber for heat generation, there is CO2 that is being generated in small amounts for the methane to reach the decomposition temperature. While this is not ideal and is the main drawback of SMR for hydrogen generation, in early simulations, Ekona found that less than 100 tonnes per day of CO2 was being generated with their PMP process as compared to the nearly 1,000 tonnes per day of CO2 being released through the SMR process as can be seen below in Figure 7.

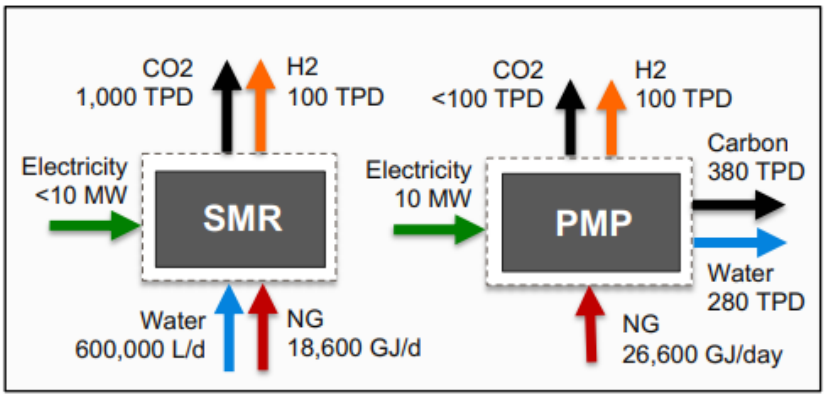

Figure 7: SMR vs Ekona's PMP

Also, comparing the two hydrogen generation processes, the SMR process requires nearly 600,000 litres per day of water to generate the steam utilized in the pyrolysis process, whereas it is estimated that the PMP process will actually generate up to 280 tonnes per day of water due to the oxidant present in the combustor. While the PMP process is more expensive due to the energy consumption

being higher than SMR, the generated carbon black through the PMP process will add more economic input to offset the higher energy costs.

Due to how new the pyrolysis process is, and even more so with Ekona's novel PMP process, there are still many unknowns about the quantity and quality of generated products. Simulation work must be completed to gain a better understanding of the trends in formation of key particles during the methane pyrolysis process.

CHAPTER 3
CHEMICAL MECHANISMS

3.1 Chemical Mechanisms

Computational modelling is a very integral, low-cost and efficient method in optimizing the yield of carbon black and other wanted particles from a pyrolysis reaction. There are many ways in which chemical kinetics of particles can be modeled with varying software. The method that was selected for this research was to run several chemical mechanisms that are available in literature through a python terminal activating a chemical kinetics library for the simulation. Each of these steps will be explained in further detail throughout this chapter.

A chemical mechanism is an input file that is interpreted by a chemical kinetics model. It is composed of three overlapping sections: the chemical data, the thermal data, and the transport data. The chemical data highlights the chemical species that are present in each mechanism, their chemical composition, and all the reactions, including reversible reactions, that the species are able to undergo. The thermal data highlights the species' thermodynamic properties through a given parametrization model as well as the temperature ranges that they can be applied in. Finally, the transport data highlights specific characteristics about the atoms or molecules and their configuration such as their geometry, well-depth, particle diameter, and polarizability.

```
- name: H2
  composition: {H: 2}
  thermo:
    model: NASA7
    temperature-ranges: [200.0, 1000.0, 3500.0]
    data:
    - [2.34433112, 7.98052075e-03, -1.9478151e-05, 2.01572094e-08, -7.37611761e-12,
      -917.935173, 0.683010238]
    - [3.3372792, -4.94024731e-05, 4.99456778e-07, -1.79566394e-10, 2.00255376e-14,
      -950.158922, -3.20502331]
    note: TPIS78
  transport:
    model: gas
    geometry: linear
    well-depth: 38.0
    diameter: 2.92
    polarizability: 0.79
```

Figure 8: Species Data for H2 Gas in ABF Mechanism

There are many different chemical mechanisms that are available in literature that all have their distinct uses and specialities, and for this reason, six different mechanisms were selected to run Ekona's new methane pyrolysis process. These six mechanisms are: ABF, Caltech_OuT, Caltech_v2.3, CRECK_2003_TOT_HT_LT, DLR and KAUST_II_Mech.

The ABF mechanism utilized in this paper is a modified version of the chemical mechanism GRI-Mech 1.2 [39], which has been utilized for many years in a wide range of studies. This modified mechanism has a total of 5 base elements including: carbon, hydrogen, oxygen, nitrogen and argon; 102 species and 544 reactions, making it the mechanism with the smallest number of reactions. Its modifications were specifically made to study soot formation in a variety of scenarios [36]. This leads to the question of if the mechanism will underperform compared with the other mechanisms in analyzing species other than carbon black.

The two Caltech mechanisms to be tested in this study are Caltech_UoT and Caltech_v2.3. Although these two mechanisms were treated as two separate mechanisms early on in the paper, it was discovered that they share the exact same species and reactions, just have differing names. These mechanisms share the base elements that were present in the ABF mechanism, however, they have 192 species and 1156 reactions. This mechanism, referred to as the Caltech mechanism in this paper, has been tested in several configurations including laminar premixed flames and laminar diffusion flames [38]. However, similarly to the other literature mechanisms tested in this paper, it has not been rigorously tested in a methane pyrolysis setting.

The CRECK_2003_TOT_HT_LT [31, 32, 33], or simply referred to as the CRECK mechanism in this paper, is an older mechanism that has been utilized for many years in combustion study work. With 6 base elements including: carbon, hydrogen, oxygen, nitrogen, argon and helium; 492

species and 17,790 reactions, this is the largest mechanism, in terms of both number of species and reactions, that will be tested in this paper. With more species and reactions present than any of the other mechanisms it will be qualitatively compared to, it leads to the question of if having more precursor species present will lead to drastically different results. This would need to occur to offset the length of time that running this large mechanism takes compared to the other smaller mechanisms.

The DLR mechanism utilized in this study is a modified version of the DLR SynNG mechanism that was utilized in modelling PAH formation in ethyl and ethane flames [34,35]. This mechanism has 6 base elements including: carbon, hydrogen, oxygen, nitrogen, argon and helium; 93 species and 719 reactions, making it the mechanism with the smallest number of species that will be tested in this paper. This leads to the question of whether having less species than the other mechanisms will lead to worse or drastically different results.

The KAUST_II_Mech, hereafter known as the KAUST mechanism in this paper, is a modified mechanism created by the King Abdullah University of Science and Technology using the USC mech version 2 [40] as the base mechanism. The KAUST mechanism, having the same 5 base elements as the ABF and Caltech mechanisms, has 202 species and 1351 reactions, thus making it the second largest mechanism tested in this paper in both number of species and reactions. This mechanism focuses on PAH formation past the conventionally simulated species, with its largest PAH simulated being coronene (C24H12).

Finally, a modified version of the ABF mechanism was created for this paper in partnership with a version of the ABF mechanism modified by researchers at Princeton University and the base ABF mechanism. The new mechanism, ABF-P utilizes the same base 5 elements of the ABF mechanism, however ABF-P has 117 species and 564 reactions, making it slightly larger than its

precursor mechanism. The main difference between the two mechanisms is the integration of a number of variations in the polycyclic aromatic hydrocarbons, or PAH, configurations and their respective reactions. An example of this would be the PAH A2R5-3. This is a nearly identical species to A2R5- which is found in both ABF and ABF-P; however, it has differing transport data as its linearity and particle diameters are different. The inclusion of these various PAH configurations may not cause a large variance in performance of methane decomposition and hydrogen generation; however, a bigger difference may be observed in the inception of carbon black as differing pathways are available in the ABF-P simulations.

3.2 Modifications Made to the Literature Mechanisms

As these chemical mechanisms have been used in literature for many years before their use in this research, they were originally found in an older file format known as Chemkin. Chemkin is a commercialized chemical kinetics model that is extremely expensive to acquire. Since one of the main goals of this research was to minimize the costs of running effective and efficient chemical kinetics simulations for the methane pyrolysis processes, a cheaper alternative model was required for this study. Cantera is an open-source model that is designed to handle problems involving thermodynamic, chemical kinetic and transport processes with applications in combustion, plasmas, detonations and many other scenarios. Cantera is a well-established and trusted simulation model that has been utilized in the combustion field for many years, giving validation to the qualitative comparison in its results. Due to Cantera being an open-source kinetics software, the overall cost of running the simulations dropped drastically compared to if the original Chemkin files would have been used. In order to make the mechanisms viable for use in the selected kinetics model of Cantera, they would need to be translated from Chemkin files into .YAML files. Chemkin

utilizes three separate files for the data necessary as inputs to run a mechanism, these three being the chemical input file (chem.inp), the thermal data (therm.dat) file, and the transport (tran.dat) file. The chemical input file is responsible for feeding the model with the needed chemical information such as species name, formation and reaction equations. The thermal data file is the source of all the thermodynamic data required by the kinetics model. Finally, the transport data file is responsible for giving the configuration specifications of the atoms or molecules that are present in the chemical input file.

For the Chemkin files to be read by Cantera, the three separate input files would need to be combined into one singular .YAML file. Fortunately, Cantera does have a Chemkin file translator built into the software, however it is not the most accurate tool. In some cases, species were left without chemical or transport data which needed to be resolved. The most troublesome portion of the translation for each of the mechanisms was in the PAH. Initially, testing of the mechanisms was to be completed through a kinetics model using Cantera developed by Ekona called the Pulsed Methane Pyrolysis Once Through Kinetics (PMP-OTK) model. This model utilized many different files that needed to highlight specific PAH as they are very important to the carbon black formation process as shown below in Figure 9. PAH are known as the precursors to carbon black formation, so it is very important for a model wanting to understand the carbon black yield quality and quantity to be focused on PAH formation.

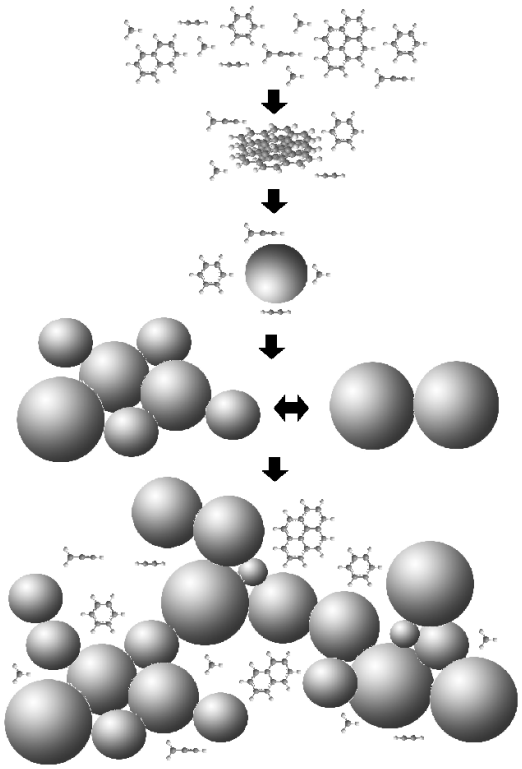

Figure 9: Formation of Carbon Black from PAH

In the OTK code, the Particle Model needed to know the indexes of certain PAH species in the mechanism, however, the naming convention amongst the mechanisms and the index present in the Particle Model did not match. Many of the chemical mechanisms have the chemical formula representations of each species; for example, benzene would be represented by its chemical composition of C6H6. In the Particle Model index, benzene was represented by the name of A1 due to the number of aromatic (6-carboned) rings present in the species. This would continue for naphthalene (C10H8) being represented by A2, phenanthrene (C14H10) being represented by A3, and pyrene (C16H10) being represented by A4. Further designations within the PAH were found such as in the case of acephenanthrene (C16H12) would be indexed as A3R5 due to the 5-carboned ring attached to the PAH, rather than being represented by its chemical formula. The final issue with the PMP-OTK mechanism translation was that the number of species present in each of the

mechanisms varied. This meant that the number of specific PAH present in each of the mechanisms would be different compared with each other as well as the index in the model code. To fix this, tailored versions of the PMP-OTK Particle Model file were made to fit the chemical nomenclature and species lists found in each of the mechanisms. This allowed all seven of the literature mechanisms to function within the Cantera model simulating the new methane pyrolysis process.

3.3 Omnisoot

Initial simulations were completed using the PMP-OTK model to ensure that all seven of the mechanisms were functional at an over-arching level, however, further specifications into desired particles called for a new Cantera model to be implemented and tested. Omnisoot is an open-source monodisperse population balance model (MDM) that is specialized in simulating low-dimensional reactors and carbon black formation. To run the MDM and Cantera in a single model, a Jupyter Notebook was created that would integrate both of the kinetics models in a single simulation through its activation in a Python Command Terminal. Similar to the PMP-OTK model, a Jupyter Notebook was tailored to each of the seven mechanisms so that their specific PAH precursor species' nomenclature and lists were present in the code index.

```
soot.set_precursor_names(['A2', 'A2R5', 'A3', 'A4'])
```

Figure 10: PAH Index in ABF Mechanism Jupyter Notebook

```
soot.set_precursor_names(['C10H8', 'C12H8', 'C14H10', 'C16H10', 'BIN1A', 'BIN1B'])
```

Figure 11: PAH Index in CRECK Mechanism Jupyter Notebook

As mentioned previously, to run the finalized simulation, a Python Terminal Command window must be run. A chemical table must be then activated using the command line:

activate ct-env

This will then set up a pre-established environment in which the Jupyter Notebook can then be called with Cantera and Omnisoot once in the proper directory using the command line:

jupyter notebook

This will then open the Jupyter Notebook file where the simulation can be run. The first block of code is the importation of all the kinetic models that we want to be present while running the simulation.

```
import cantera as ct
from omnisoot import ConstantVolumeReactor, SootGas, SootThermo
import numpy as np
import os
import pandas as pd
import time
```

Figure 12: Importation of Desired Models in Jupyter Notebook

This will establish the chemical table, the reactor parameters and the MDM for soot growth from Omnisoot, array calculations through the Python library Numpy, and data structure and analysis tools from the Python package Pandas. Next, the chemical mechanism is called to the models as well as a Pre-Pyrolysis text file that specifies the mass concentrations of the input species entering in the methane pyrolysis chamber.

```
gas = ct.Solution('ABF-P.yaml')
```

Figure 13: Calling of ABF Mechanism in the Jupyter Notebook

Further specifications such as reactor temperature, reactor pressure and residence time can be modified from this Jupyter Notebook. Once all the parameters are set and the Notebook is run, the final results are printed out in large Microsoft Excel files for analysis.

CHAPTER 4
SIMULATIONS AND RESULTS

4.1 Simulation Boundaries

Since the modified literature mechanisms had not been rigorously tested in a methane pyrolysis setting before, a large sample size of simulations was set up to understand how the performance of each mechanism would vary for a given range of temperatures, pressures and reactor residence times. Methane pyrolysis usually takes place above 1000°C, or about 1273K, so a temperature range of 700K to 2000K in increments of 100K was decided for the simulation work. While the temperature range began much lower than the temperature in which pyrolysis would occur, it provided the opportunity to explore the impact of other inputs and how they would affect the initial decomposition temperature. Next, a pressure range of 2-Bar to 40-Bar in increments of 3-Bar was decided for the research. It was important in this qualitative study to understand the impact of pressure on the overall effectiveness of the pyrolysis process and to see if the initial decomposition temperature would be affected drastically by a varying pressure. Ekona estimated that they would run their pyrolysis reaction chamber at approximately 12-Bar, however, having the capability of running at higher pressures, a large range above and below this operating pressure was selected. Finally, three residence times were decided for the experiment: 0.1 seconds, 0.5 seconds and 1 second. Due to how quick the reaction occurs in the pulsed methane pyrolysis chamber stetting; the residence time did not have a significant impact on the simulation results.

With these three key input ranges selected, the modified literature mechanisms would be qualitatively compared with each other to understand how and when they should be utilized in a methane pyrolysis setting. Another key detail about these simulations is that the Pre-Pyrolysis input text file was loaded with a mass concentration of purely methane. This is specified because

Ekona's PMP process will have other gases that are present during the transfer from the combustion chamber to the pyrolysis chamber. For this study, only methane is considered as an input due to wanting to understand the differences in functionality of the literature mechanisms in a pyrolysis setting. Therefore, we are not concerned about the extra inputs that are present specifically in Ekona's PMP process, only the pyrolyzing methane is of concern. The first measure to be tested was the rate of methane decomposition. Since the only gas present in the input file is methane, looking into its rate of decomposition will give a clear analysis of how the gases in the PMP system will react, as well as give an indication of how hydrogen gas will be generated since this is the only major gas that will be forming in these trials.

4.2 Methane Decomposition Comparison

The first input range to be tested amongst the literature mechanisms was the temperature range. All the chemical mechanisms were run from 700K to 2000K at intervals of 100K to see which mechanism would show signs of methane decomposition first. The residence time was selected to be maintained at 0.1 seconds as this allowed for the most efficient simulation process for the temperature study. The comparison was completed at 12-Bar as this was the pressure in which Ekona was estimating to be the functional pyrolysis chamber pressure. Seen below in Table 1 is the summary comparison of the temperatures in which the methane decomposed to specific percentages of its initial mass concentration.

Mechanism	Temperature (K) at 99%	Temperature (K) at 90%
ABF	1300-1400	1400-1500
Caltech	1300-1400	1300-1400
DLR	1300-1400	1300-1400
KAUST	1300-1400	1400-1500
CRECK	1300-1400	1300-1400
ABF-P	1300-1400	1400-1500

Table 1: Methane Decomposition Temperature Comparison at 12-Bar

The first methane decomposition percentage that was selected for trial was when the methane achieved a mass concentration of 99 percent. This percentage was selected since this allows us to gain an understanding of when the pyrolysis process truly begins. Looking at the results, the pyrolysis process begins between 1300K to 1400K for all 7 of the literature mechanisms. This is an expected result as the methane should begin pyrolyzing at roughly the same temperature in each of the simulations. However, the rate at which the methane will pyrolyze will be different due to the differing species present in each of the mechanisms. This can be seen as the methane mass concentration approaches the next chosen percentage of 90 percent. There are four mechanisms that achieve the 90 percent methane mass concentration between the temperatures of 1300 K and 1400K whereas the remaining three mechanisms do not reach the 90 percent mark until between the temperatures of 1400K and 1500K. The three mechanisms that achieved the 90 percent methane concentration at a higher temperature range are ABF, ABF-P and KAUST. This leads

into an investigation to how the mechanisms will simulate pyrolysis under various pressure conditions within the PMP reactor chamber.

Next, a comparison was completed looking at how differing pressures affected the temperatures in which methane decomposition first begins in the PMP reactor. The same methane mass concentration percentages were chosen for the comparison, however, the pressures of 2-Bar, the lowest of the pressure range, and 40-Bar, the highest of the pressure range were selected to be compared with each other as well as the 12-Bar results from the previous comparison. Shown below in Tables 2 and 3 are the comparison of when the methane mass concentration decreased to 99 percent of its original mass and 90 percent of its original mass at both 2-Bar and 40-Bar pressures respectively.

Mechanism	Temperature at 99% (K)	Temperature at 90% (K)
ABF	1300-1400	1400-1500
Caltech	1300-1400	1400-1500
DLR	1400-1500	1400-1500
KAUST	1300-1400	1400-1500
CRECK	1300-1400	1400-1500
ABF-P	1300-1400	1400-1500

Table 2: Methane Decomposition Temperature Comparison at 2-Bar

Mechanism	Temperature at 99% (K)	Temperature at 90% (K)
ABF	1300-1400	1400-1500
Caltech	1200-1300	1300-1400
DLR	1200-1300	1300-1400
KAUST	1300-1400	1300-1400
CRECK	1300-1400	1300-1400
ABF-P	1300-1400	1400-1500

Table 3: Methane Decomposition Temperature Comparison at 40-Bar

Trends in the mechanisms can be seen in the above tables as the temperature ranges in which the methane decreased to 99 percent of its original mass concentration increased at a lower pressure and decreased at a higher pressure. This was shown in an increase in temperature range in the DLR simulation at 2-Bar, and with a decrease for two mechanisms, Caltech and DLR, at 40-Bar. This displays a connection between the pressure and the temperature in which pyrolysis first occurs within a time frame of 0.1 seconds. Looking further at the methane at 90 percent of its original mass concentration, all the mechanisms achieved this in the 1400K to 1500K range in the 2-Bar trial. Compared with the 12-Bar and 40-Bar trials, several of the mechanisms achieved the 90 percent methane concentration in the 1300K to 1400K range. This demonstrates a relationship between the initial conversion rate of methane at a specific temperature and pressure. At an elevated pressure, the temperature range in which methane initially is decomposed decreases compared to a relatively lower pressure.

This comparison was continued further to see how the chamber pressure affected methane decomposition throughout the entire temperature range. Shown below in Figure 14 is the mass concentration of methane at 2-Bar throughout the temperature range of 1200K to 2000K.

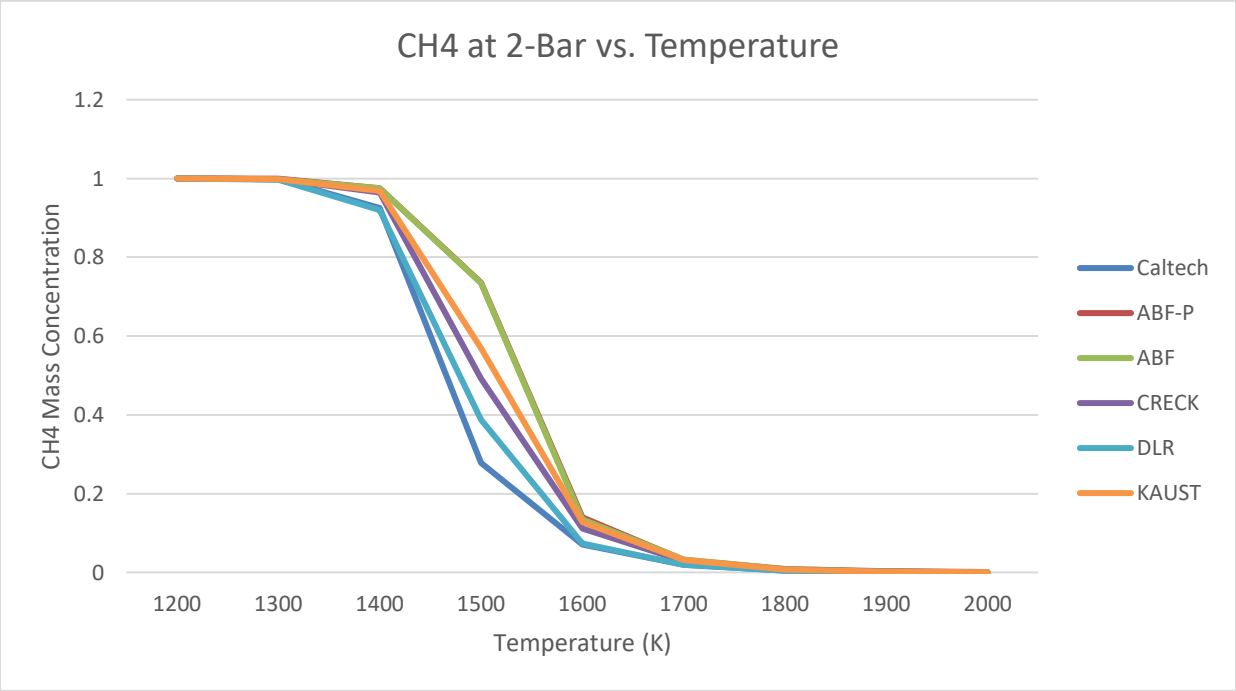

Figure 14: Methane Decomposition Temperature Comparison at 2-Bar

The temperature range of 1200K to 2000K was selected due to this being the temperatures in which the methane was proven to begin pyrolyzing. Next, the mass concentration of methane at 40-Bar throughout the same temperature range of 1200K to 2000K is shown below in Figure 15.

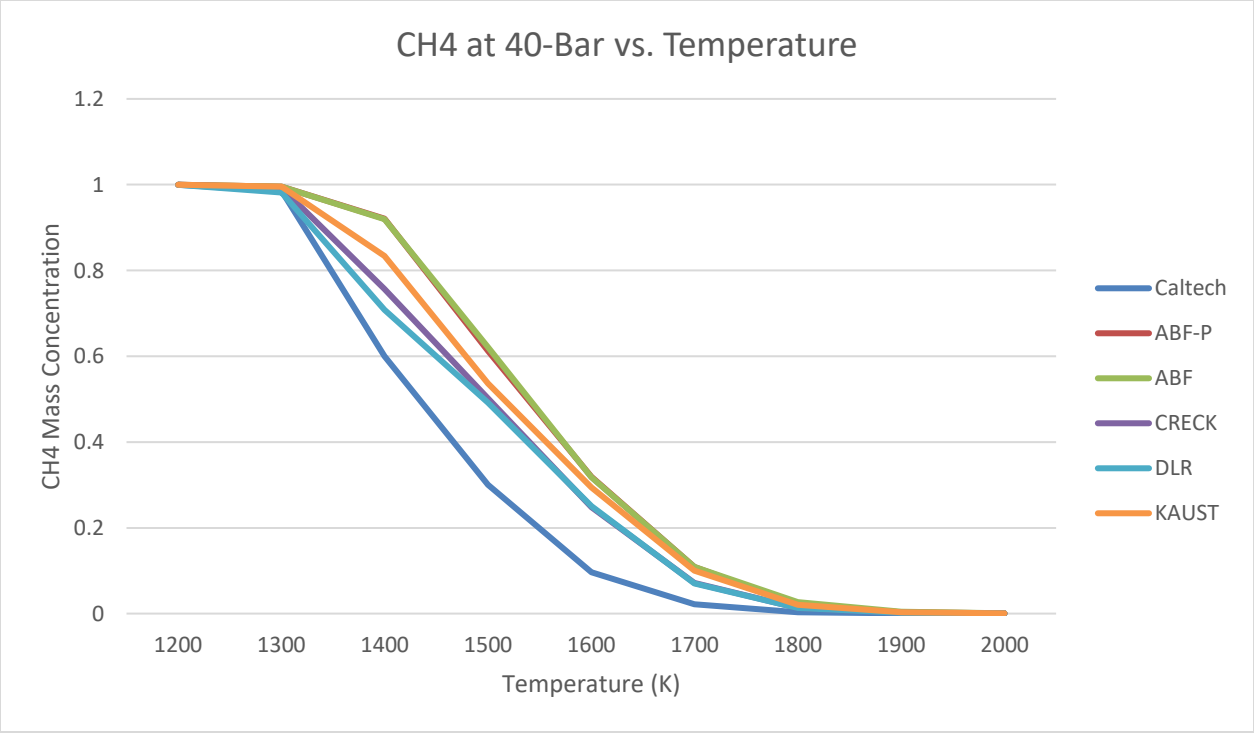

Figure 15: Methane Decomposition Temperature Comparison at 40-Bar

Comparing the two graphs, there are clear distinctions between the presence of methane at 2-Bar and 40-Bar after undergoing the PMP process at a variety of temperatures. The first major difference between the mass concentration at 2-Bar and 40-Bar is the rate of decomposition. While methane begins decomposing at a lower temperature at 40-Bar as compared to at 2-Bar, the rate at which the methane decreases is higher for the 2-Bar trial. This can be seen by the average methane concentration at 1400K for the 40-Bar trial being much lower than that of the 2-Bar trial, while the average methane concentration at 1600K for the 2-Bar is much lower than that of the 40-Bar. This could lead to the result that although methane begins decomposing at an earlier temperature at high pressures, the methane undergoes a more complete and efficient pyrolysis reaction at lower pressures. This can be further demonstrated at the higher pyrolysis temperatures. Complete pyrolysis occurs at roughly 1800K for the 2-Bar trial, whereas in the 40-Bar trial there are still many mechanisms that have methane present in a substantial amount at that same temperature.

This could mean that there is a diminishing return for increased pressure in a pyrolysis system. While the increased pressure could act similarly to a catalyst and lower the reaction temperature where pyrolysis first begins, it could have a negative effect on the overall efficacy of the pyrolysis process in the PMP reactor.

Finally, looking at the mechanism comparison, clear best-case and worst-case scenarios can be observed in PMP methane decomposition. Between the temperatures of 700K and 1300K, the mechanisms behave relatively the same for both high and low pressures. For the low-pressure trial, between the temperatures of 1300K and 1600K, DLR and Caltech are the best-case scenarios in which the most methane decomposes. ABF and ABF-P would be considered the worst-case scenario as they have the worst methane conversion as compared to the other mechanisms in this same temperature range. Between the temperatures of 1600K and 1700K, ABF and ABF-P converge with the rest of the mechanisms other than DLR and Caltech, thus continuing the trend of the latter two as simulating the best case-scenario for methane decomposition at lower pressure. Finally, past 1700K, all the mechanisms converge as there is very little to no methane present. For the high-pressure trial, there are very similar trends in best-case and worst-case scenarios. Between the temperatures of 700K and 1300K, the mechanisms behave very similarly as there is very little methane decomposition present. Between the temperatures of 1300K and 1600K, the best-case scenario for methane conversion in the PMP process is simulated by the Caltech mechanism, while the worst-case scenario is simulated by ABF and ABF-P. During this temperature range, Caltech is a clear outlier compared with the other mechanisms, so it is possible that it is actually over-predicting the decomposition of methane during these temperatures. This is especially shown at 1600K, Caltech is simulating a mass concentration level of 0.096, whereas the rest of the mechanisms are simulating a mass concentration level in the 0.2-0.4 range. In the temperature

range of 1600K to 1900K, the ABF and ABF-P mechanisms converge with the KAUST and CRECK mechanisms forming the worst-case scenario while Caltech remains the best-case scenario simulation. Past 1900K, all the mechanisms converge as complete pyrolysis occurs and little to no methane is present in the PMP chamber. These trends in the best-case and worst-case scenarios show that for a large range of temperatures in both high and low pressure settings, results from simulations using the Caltech mechanism show the best-case methane conversion rates. The same can be said as the worst-case scenarios in both high and low pressure settings were found through the simulation results of the ABF and ABF-P mechanisms. Although they predicted the worst methane conversion compared to the other mechanisms, it does not mean that these simulations are the worst results. As mentioned previously, it is possible that the best-case scenarios were greatly over-predicting the rate of methane decomposition. In this qualitative comparison, trends are found to gain a better understanding of when to utilize given mechanisms for desired simulation results. If best case-scenario results wished to be acquired for methane decomposition in the PMP reactor at a given temperature, then no other mechanism other than Caltech would need to be run for the given case. However, if a more conservative and possibly more realistic approach would want to be taken, and simulations of the worst-case scenario were needed, then no other mechanism besides ABF/ABF-P would need to be run. This availability of selectivity decreases the overall computational cost and time.

4.3 Hydrogen Gas Production Comparison

A continuation of the qualitative modified literature mechanism testing would have the mechanisms undergo the same trial conditions, a temperature range of 700K to 2000K and a pressure range of 2-Bar to 40-Bar, however a focus was put on the rate of hydrogen gas production.

Found in Appendix A, the comparison tables (Table A-1 and Table A-2) display the temperature ranges in which hydrogen gas mass concentrations achieve a concentration of 1 percent in chamber pressure situations of 2-Bar and 40-Bar. In the 2-Bar situation, all six of the mechanisms tested achieved a mass concentration level of 1 percent in the temperature range of 1300K to 1400K. In the 40-Bar simulation, only Caltech and DLR were able to achieve a hydrogen gas mass concentration at a lower temperature range of 1200K to 1300K, whereas the remaining mechanisms achieved this concentration at the same temperature range as before at 1300K to 1400K. Since the temperature ranges of hydrogen gas production began at 1200K, a further analysis on the mechanism performance between the temperatures of 1200K and 2000K for both the 2-Bar and 40-Bar scenarios was performed. This can be seen below in Figures 16 and 17 for the 2-Bar and 40-Bar trials respectively.

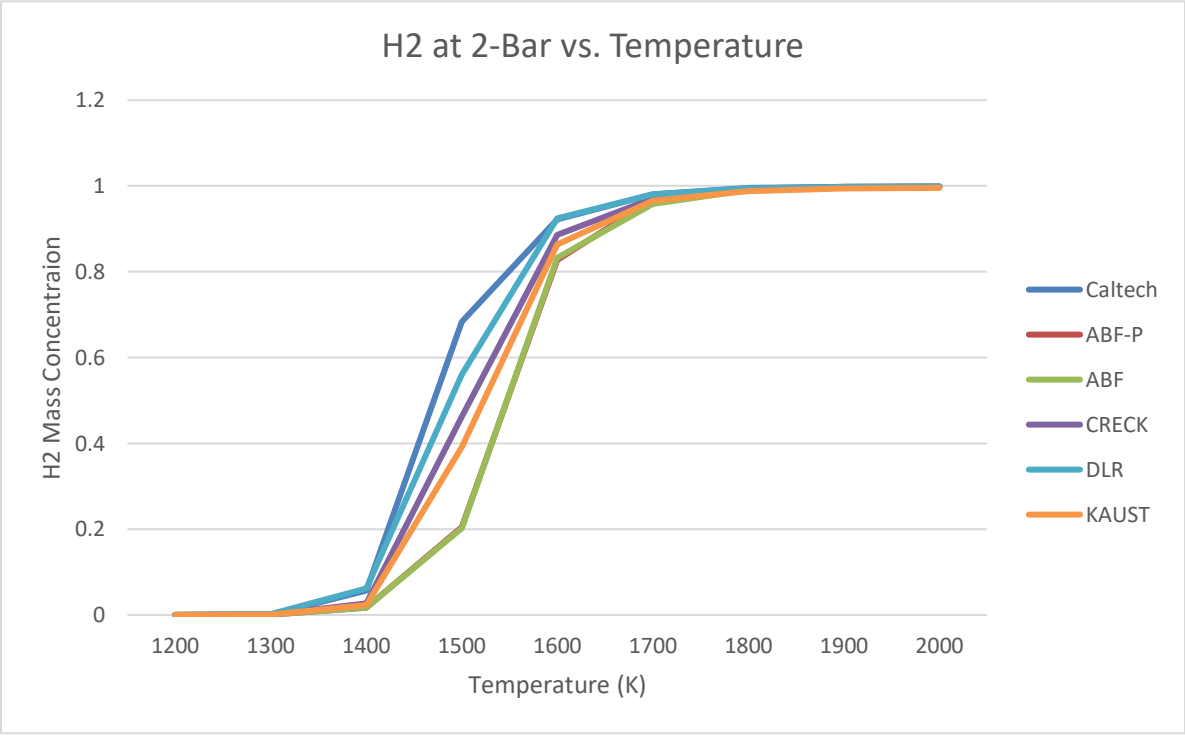

Figure 16: Hydrogen Gas Production Temperature Comparison at 2-Bar

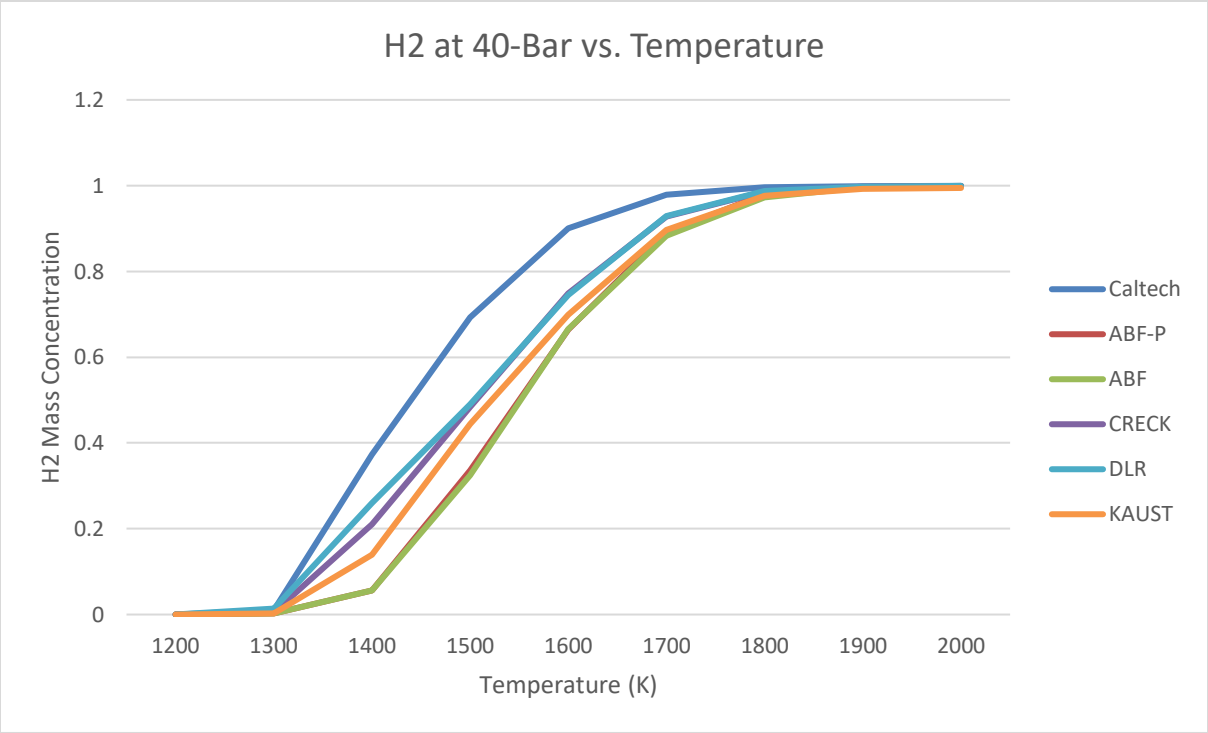

Figure 17: Hydrogen Gas Production Temperature Comparison at 40-Bar

Looking at the two graphs, trends can be also found in the production of hydrogen gas in both the 2-Bar and the 40-Bar simulations. Comparing the mechanisms in the 2-Bar scenario, from 700K to 1300K, all the mechanisms behave the same as there is very little to no hydrogen gas being produced. Between the temperatures of 1300K and 1400K, DLR would be considered best-case scenario, however, there is not a drastic difference in hydrogen produced compared to the other mechanisms. From 1400K to 1600K, Caltech simulates the best-case scenario of hydrogen gas generation while ABF and ABF-P simulate the worst-case scenarios. Between 1600K and 1700K, DLR becomes the new best-case scenario once more for hydrogen gas generation while ABF and ABF-P remain the worst-case scenario. From 1700K to 1800K, ABF and ABF-P converge with the other mechanisms, leaving only DLR as the best-case scenario. Finally, past 1800K, DLR

converges with the rest of the mechanisms as hydrogen gas takes up a large majority of the gas mass concentration. This is due to there being very little methane left to break down and form the hydrogen gas. For the high-pressure test, there are similar trends as with the low-pressure test, with some key differences. Similar to the low-pressure test, there is very little to no hydrogen being produced under 1200K, so there is no difference in mechanism simulation. Between the temperatures of 1200K and 1300K, DLR and Caltech are the best-case scenario by very small margin as there is very little to no hydrogen production present in the other simulations. From 1300K to 1600K, Caltech is a clear outlier as the best-case scenario, while ABF and ABF-P are the worst case-scenario simulations. Between the temperatures of 1600K and 1700K, Caltech is still the best-case simulation, whereas ABF, ABF-P and KAUST converge to form the worst-case scenario. Between 1700K and 1800K, DLR converges with the rest of the mechanisms, leaving solely Caltech as the only outlier until it finally converges with the rest of the mechanisms past 1800K. Past 1800K, there is very little difference between the mechanisms as there is little to no more hydrogen gas being generated.

Looking at these comparison graphs, there are many trends that can be found. The overall trend of reaction rate between the low-pressure and the high-pressure settings appears to share similarities between methane decomposition and hydrogen gas formation. This is an expected result as these are the only two major gases that are present in the reaction with methane being the only input gas. Similarly to the rate of methane decomposition, the hydrogen gas formation begins at lower temperatures in a higher-pressure environment. While this is true, the rate at which the hydrogen is generated appears to be faster in the lower pressure setting as compared with the higher-pressure setting. This can be seen by observing the hydrogen gas mass concentrations at 1600K in both the low and high pressure environments. In the low-pressure trial, the average mass concentration is

in the range of 0.8-1 whereas in the high-pressure trial, the average mass concentration is in the range of 0.6-0.8 excluding the outlier of Caltech. This again shows that while there is an early advantage in PMP reaction at higher pressures, the overall reaction appears to perform more effectively at a relatively lower pressure.

In high and low temperatures settings in the 2-Bar pressure trial, DLR was found to be best-case scenario, whereas any of the other mechanisms other than Caltech could be utilized as the worst-case scenario. In the mid-range temperatures, Caltech was found to be best-case scenario, while ABF and ABF-P were found to be the worst-case scenario. Finally, looking at the high-pressure setting, there is a continued trend present with the Caltech mechanism. In both the high-pressure results for methane decomposition and hydrogen gas generation, Caltech is a clear outlier as the best-case scenario. However, it seems as though it is over-predicting its results, in some cases drastically so. This could lead to a possible finding that the Caltech mechanism might not be a reliable best-case scenario simulation in high-pressure settings. Over-predicting results can be as harmful as under-predicting them. Further analysis into this trend would be observed in later simulations.

4.4 Carbon Black Generation Comparison

The final qualitative study that was conducted between the literature chemical mechanisms was the formation of Carbon Black. As mentioned before, along with hydrogen gas, carbon black is a paramount product of the methane pyrolysis process as it adds economic incentive to the process. To understand and predict how the carbon black was going to form, trials could be done to study the important precursors of the carbon black formation process, the PAH. There are several key PAH that are present in each of the mechanisms, and while there are similarities that are shared

amongst the PAH present, there are still many differences from mechanism to mechanism. This can be demonstrated by the largest PAH present in each of the mechanisms. In ABF, ABF-P, DLR and Caltech, the largest PAH that is present is pyrene (A4), while the largest PAH in the CRECK mechanism is BIN1A ($C_{20}H_{16}$) and coronene ($C_{24}H_{12}$) in the KAUST mechanism. While these large PAH are vital in the inception of carbon black, since they differ amongst the mechanisms, it would be nearly valueless to run a qualitative study on their formation as there is little to compare with each other. In an effort to combat this, a comparison study was completed looking at a PAH that is present in each mechanism and is still vital in the formation of carbon black: benzene or A1 (C_6H_6). The results of this trial can be seen in Appendix A (Figures A-1 and A-2), and the results are somewhat expected. Due to the differing species lists present in each of the mechanisms, there are many different pathways in which benzene could be formed. This led to no clear trends forming in terms of best-case or worst-case scenarios, as well as no clear outliers. Therefore, a final study was completed looking into the final mass concentration of carbon black formed throughout the same temperature, pressure and residence time ranges as the methane decomposition and hydrogen generation trials. While these trials were completed from 700K to 2000K, these graphs only show the temperature range of 1200K to 2000K since there was no carbon black formation before these temperatures at any tested pressure. This study can be seen below in Figures 18 and 19 for the 2-Bar and 40-Bar settings respectively.

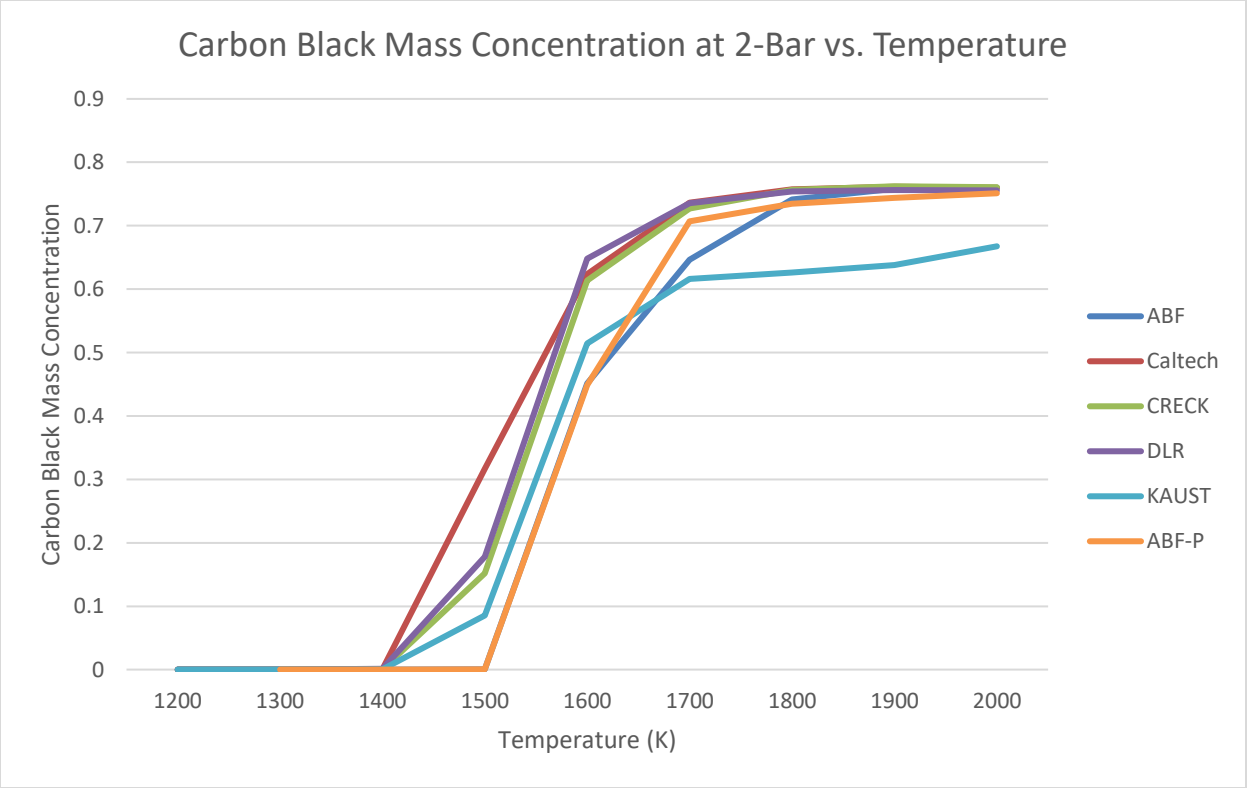

Figure 18: Carbon Black Formation Temperature Comparison at 2-Bar

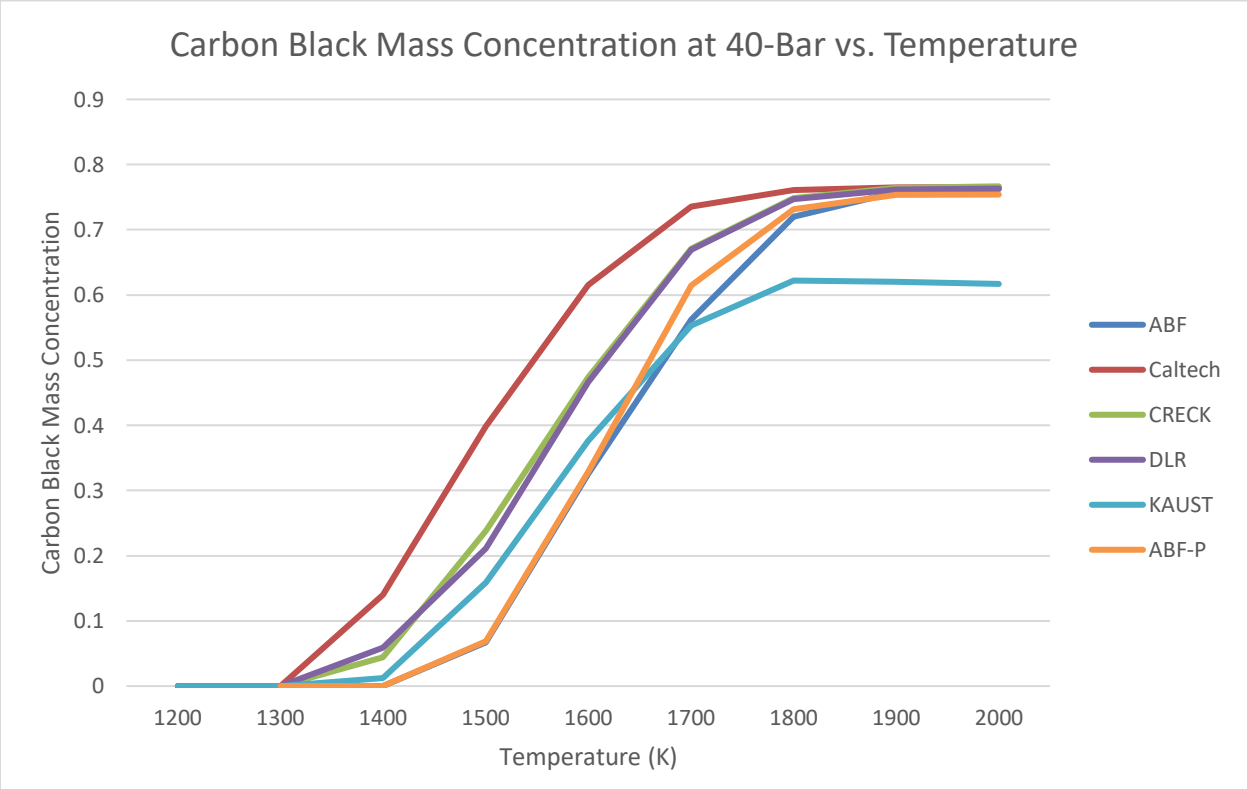

Figure 19: Carbon Black Formation Temperature Comparison at 40-Bar

Multiple new and returning trends can be seen in this trial. Looking at the low-pressure setting, there is very little carbon black formed under 1400K, therefore there is no difference in the performance of the chemical mechanisms. From 1400K to 1500K, Caltech simulates the best-case scenario while ABF and ABF-P do not demonstrate nearly any carbon black being formed. Between the temperatures of 1500K and 1600K, ABF and ABF-P continue to simulate the worst-case scenarios while Caltech simulates the best-case scenario. From 1600K to 1700K, ABF simulates the worst-case scenario and DLR simulates the new best-case scenario. Between the temperatures of 1700K and 1800K, DLR continues to simulate the best-case scenario, while KAUST simulates the new worst-case scenario. Finally past 1800K, most of the mechanisms converge while CRECK becomes the best-case scenario at high temperatures, and KAUST remaining the worst-case scenario, never converging with the rest of the mechanisms. Looking at the high-pressure scenario, from 1300K to 1400K, ABF, ABF-P and KAUST all have very little to no carbon black generation whereas Caltech has a significantly higher carbon black concentration than the other mechanisms. From 1400K to 1700K, Caltech is continually over-predicting compared with the other mechanisms while ABF and ABF-P simulate the worst-case scenario. From 1700K onwards, all the mechanisms other than KAUST converge.

Observing these results, multiple trends can be identified. The first is that ABF and ABF-P should not be used to simulate low temperature low pressure carbon black formation at short residence times as there is very little to no carbon black formation compared with every other mechanism. Secondly, the KAUST mechanism should not be utilized to simulate high temperature carbon black formation. This is because it drastically under-predicts the carbon black being formed at these high temperatures in both low and high pressure settings in the PMP reactor. Finally, once more the Caltech mechanism appears to be over-predicting yields at high pressures compared to

the other mechanisms. This continues the trend that Caltech may not be the most accurate and best-suited mechanism to use in a pyrolysis reaction simulation at high pressures.

One of the key factors affecting the increments of the simulations was the duration of the simulations. While a second pass of temperature and pressure studies in smaller increments could have led to a more refined qualitative study, the incredibly high computational time to run these added simulations would not have led to substantially better comparisons. The overall goal of the study was to lower the computational costs of running pyrolysis simulations by lowering the number of chemical mechanisms needed to effectively study particle formation and decomposition in the reaction. This goal, and more, was achieved with the set simulations and their respective computational limitations in boundaries and increments.

CHAPTER 5
CONCLUSIONS AND FUTURE WORK

5.1 Conclusions

This study successfully implements multiple literature chemical kinetics mechanisms in a pulsed methane pyrolysis setting. These chemical kinetics simulations are used to gain an understanding of the predictive performance of multiple molecules in Ekona's pulsed methane pyrolysis reactor at different temperatures, pressures and residence times. These simulations are also used to understand during what settings the different chemical mechanisms should be utilized and identify any major trends or outliers that are present throughout the temperature and pressure ranges. In conclusion, this study:

1. Implements multiple chemical kinetics mechanisms in an open-source, easily accessible, and cost-effective format for methane pyrolysis simulations.
2. Recognized a pattern in best-case scenario performances, the Caltech mechanism predicted the best-case scenario for methane decomposition, hydrogen production, and low-pressure low temperature carbon black formation.
3. Recognized a pattern in the worst-case scenario performances, the ABF and ABF-P mechanisms simulated the worst-case low temperature scenarios for methane decomposition, hydrogen production and carbon black formation.
4. Illustrates a pattern in the KAUST mechanism, that predicts lower carbon black formation at high temperatures past 1700K compared with the other mechanisms. Therefore, it may not be the best-suited mechanism to simulate carbon black formation through a large temperature range.

5. Illustrates a pattern in the Caltech mechanism, that predicts yields much greater or much lower than the other mechanisms at high pressures. Therefore, it may not be the best-suited and most accurate mechanism to be utilized in high-pressure methane pyrolysis simulations.
6. Illustrates a pattern that the pulsed methane pyrolysis process is more effective at total methane decomposition and hydrogen production at low pressures throughout the entire observed temperature range.

5.2 Future Work

Although this research paper identified key intervals in which the literature mechanisms simulate best-case and worst-case scenarios as well as specific intervals of under-predicting or over-predicting, further work should be completed to reduce simulation costs even further. To further improve upon the work in simulating the methane pyrolysis reaction, future work should be done:

1. Quantitatively compare the mechanism simulation data against experimental data from Ekona's pulsed methane pyrolysis reactor. As this study is a qualitative investigation into the trends in simulation results, further work should be conducted to validate the simulation data with real-world data.
2. Create a mechanism that is a mixture of the best-case or worst-case scenarios for all particles that are highlighted as important in the methane pyrolysis reaction. This would further decrease the simulation costs as one mechanism would be able to be run for all particle simulation through the entire range of desired pressures and temperatures, rather than utilizing specific mechanisms that were highlighted as performing well in specific intervals in this study.

REFERENCES

[1] United Nations, “Causes and effects of climate change,” *United Nations, 2023.* https://www.un.org/en/climatechange/science/causes-effects-climate-change

[2] NASA. “What Is the Greenhouse Effect?” *Science.nasa.gov*, NASA, 2024, science.nasa.gov/climate-change/faq/what-is-the-greenhouse-effect/

[3] International Energy Agency. “CO2 Emissions in 2022.” *IEA*, IEA, Mar. 2023, www.iea.org/reports/co2-emissions-in-2022.

[4] PPCA. “Overview.” *Powering Past Coal Alliance*, 2 Aug. 2022, poweringpastcoal.org/our-work/.

[5] International Energy Agency. “Emissions – Global Energy & CO2 Status Report 2019 – Analysis.” *IEA*, Mar. 2019, www.iea.org/reports/global-energy-co2-status-report-2019/emissions.

[6] N. A. Slavinskaya and P. Frank, “A modelling study of aromatic soot precursors formation in laminar methane and ethene flames,” *Combustion and Flame*, vol. 156, no. 9, pp. 1705–1722, Sep. 2009, Available: https://doi.org/10.1016/j.combustflame.2009.04.013

[7] EPA, “Sources of Greenhouse Gas Emissions,” *United States Environmental Protection Agency*, Jul. 08, 2024. https://www.epa.gov/ghgemissions/sources-greenhouse-gas-emissions

[8] Government of Canada, “Greenhouse gas emissions,” *Canada.ca*, May 02, 2024. https://www.canada.ca/en/environment-climate-change/services/environmental-indicators/greenhouse-gas-emissions.html

[9] N. R. Canada, “The Hydrogen Strategy,” *natural-resources.canada.ca*, Oct. 20, 2020. https://natural-resources.canada.ca/climate-change/canadas-green-future/the-hydrogen-strategy/23080

[10] M. M. Kuszynska, M. I. Szynkowska-Jozwik, and P. Mierczynski, “Oxy-Steam Reforming of Natural Gas on Ni Catalysts—A Minireview,” *Catalysts*, vol. 896, no. 10, Aug. 2020, doi: https://doi.org/10.3390/catal10080896.

[11] C. Hussy, “Water electrolysis explained – the basis for most Power-to-X processes,” *PtX Hub*, May 28, 2021. https://ptx-hub.org/water-electrolysis-explained/#:~:text=The%20basic%20principle%20of%20electrolysis

[12] N. Marchant, “Grey, blue, green – why are there so many colours of hydrogen?,” *World Economic Forum*, Jul. 27, 2021. https://www.weforum.org/agenda/2021/07/clean-energy-green-hydrogen/

[13] N. Sánchez-Bastardo, R. Schlögl, and H. Ruland, “Methane Pyrolysis for CO 2 -Free H 2 Production: A Green Process to Overcome Renewable Energies Unsteadiness,” *Chemie Ingenieur Technik*, vol. 92, no. 10, pp. 1596–1609, Aug. 2020, doi: https://doi.org/10.1002/cite.202000029.

[14] M. McConnachie, M. Konarova, and S. Smart, “Literature review of the catalytic pyrolysis of methane for hydrogen and carbon production,” *International Journal of Hydrogen Energy*, vol. 48, no. 66, pp. 25660–25682, Aug. 2021, doi: https://doi.org/10.1016.

[15] P. Gururani *et al.*, “Recent advances and viability in sustainable thermochemical conversion of sludge to bio-fuel production,” *Fuel*, vol. 316, no. ScienceDirect, p. 123351, May 2022, doi: https://doi.org/10.1016/j.fuel.2022.123351.

[16] Plasma Science and Fusion Center Massachusetts Institute of Science and Technology, “What is Plasma? ,” *MIT Plasma Science and Fusion Center*, 2020. https://www.psfc.mit.edu/vision/what_is_plasma

[17] M. Wnukowski, “Methane Pyrolysis with the Use of Plasma: Review of Plasma Reactors and Process Products,” *Energies*, vol. 16, no. 18, p. 6441, Jan. 2023, doi: https://doi.org/10.3390/en16186441.

[18] A. Punia, J. Tatum, L. Kostiuk, J. Olfert, and M. Secanell, “Analysis of methane pyrolysis experiments at high pressure using available reactor models,” *Chemical Engineering Journal*, vol. 471, p. 144183, Sep. 2023, doi: https://doi.org/10.1016/j.cej.2023.144183.

[19] S. R. Patlolla, K. Katsu, A. Sharafian, K. Wei, O. E. Herrera, and W. Mérida, “A review of methane pyrolysis technologies for hydrogen production,” *Renewable and Sustainable Energy Reviews*, vol. 181, p. 113323, Jul. 2023, doi: https://doi.org/10.1016/j.rser.2023.113323.

[20] M. R. Kholghy and G. A. Kelesidis, “Surface growth, coagulation and oxidation of soot by a monodisperse population balance model,” *Combustion and Flame*, vol. 227, pp. 456–463, May 2021, doi: https://doi.org/10.1016/j.combustflame.2021.01.010.

[21] S. Peukert *et al.*, “The influence of hydrogen and methane on the growth of carbon particles during acetylene pyrolysis in a burnt-gas flow reactor,” *Proceedings of the Combustion Institute*, vol. 37, no. 1, pp. 1125–1132, 2019, doi: https://doi.org/10.1016/j.proci.2018.05.049.

[22] Q. Wang *et al.*, “Effect of pressure on the pyrolysis and gasification mechanism of corn stovers from kinetics,” *Journal of Analytical and Applied Pyrolysis*, vol. 176, p. 106267, Nov. 2023, doi: https://doi.org/10.1016/j.jaap.2023.106267.

[23] G. A. Kelesidis and M. R. Kholghy, “A Monodisperse Population Balance Model for Nanoparticle Agglomeration in the Transition Regime,” *Materials*, vol. 14, no. 14, p. 3882, Jul. 2021, doi: https://doi.org/10.3390/ma14143882.

[24] A. Naseri, M. R. Kholghy, N. A. Juan, and M. J. Thomson, “Simulating yield and morphology of carbonaceous nanoparticles during fuel pyrolysis in laminar flow reactors enabled by reactive inception and aromatic adsorption,” *Combustion and Flame*, vol. 237, p. 111721, Mar. 2022, doi: https://doi.org/10.1016/j.combustflame.2021.111721.

[25] M. R. Kholghy *et al.*, “Comparison of multiple diagnostic techniques to study soot formation and morphology in a diffusion flame,” *Combustion and Flame*, vol. 176, pp. 567–583, Feb. 2017, doi: https://doi.org/10.1016/j.combustflame.2016.11.012.

[26] M. E. Mueller, G. Blanquart, and H. Pitsch, “Hybrid Method of Moments for modeling soot formation and growth,” *Combustion and Flame*, vol. 156, no. 6, pp. 1143–1155, Jun. 2009, doi: https://doi.org/10.1016/j.combustflame.2009.01.025.

[27] S. Wu *et al.*, “A moment projection method for population balance dynamics with a shrinkage term,” *Journal of Computational Physics*, vol. 330, pp. 960–980, Feb. 2017, doi: https://doi.org/10.1016/j.jcp.2016.10.030.

[28] A. B. Shirsath *et al.*, “Soot Formation in Methane Pyrolysis Reactor: Modeling Soot Growth and Particle Characterization,” *Journal of Physical Chemistry A*, vol. 127, no. 9, pp. 2136–2147, Feb. 2023, doi: https://doi.org/10.1021/acs.jpca.2c06878

[29] M. Mokashi *et al.*, “Understanding of gas-phase methane pyrolysis towards hydrogen and solid carbon with detailed kinetic simulations and experiments,” *Chemical Engineering Journal*, vol. 479, p. 147556, Jan. 2024, doi: https://doi.org/10.1016/j.cej.2023.147556.

[30] P. Lott *et al.*, “Hydrogen Production and Carbon Capture by Gas-Phase Methane Pyrolysis: A Feasibility Study,” *ChemSusChem*, vol. 16, no. 6, Dec. 2022, doi: https://doi.org/10.1002/cssc.202201720.

[31] E. Ranzi, A. Frassoldati, A. Stagni, M. Pelucchi, A. Cuoci, and TI. Faravelli, “Reduced Kinetic Schemes of Complex Reaction Systems: Fossil and Biomass-Derived Transportation Fuels,” *International Journal of Chemical Kinetics*, vol. 46, no. 9, pp. 512–542, Jul. 2014, doi: https://doi.org/10.1002/kin.20867.

[32] E. Ranzi, C. Cavallotti, A. Cuoci, A. Frassoldati, M. Pelucchi, and T. Faravelli, “New reaction classes in the kinetic modeling of low temperature oxidation of n-alkanes,” *Combustion and Flame*, vol. 162, no. 5, pp. 1679–1691, May 2015, doi: https://doi.org/10.1016/j.combustflame.2014.11.030.

[33] G. Bagheri, E. Ranzi, M. Pelucchi, A. Parente, A. Frassoldati, and T. Faravelli, “Comprehensive kinetic study of combustion technologies for low environmental impact: MILD and OXY-fuel combustion of methane,” *Combustion and Flame*, vol. 212, pp. 142–155, Feb. 2020, doi: https://doi.org/10.1016/j.combustflame.2019.10.014.

[34] S. B. Dworkin, Q. Zhang, M. J. Thomson, N. A. Slavinskaya, and U. Riedel, "Application of an enhanced PAH growth model to soot formation in a laminar coflow ethylene/air diffusion flame," *Combustion and Flame*, vol. 158, no. 9, pp. 1682–1695, Sep. 2011, doi: https://doi.org/10.1016/j.combustflame.2011.01.013.

[35] N. A. Slavinskaya, U. Riedel, S. B. Dworkin, and M. J. Thomson, "Detailed numerical modeling of PAH formation and growth in non-premixed ethylene and ethane flames," *Combustion and Flame*, vol. 159, no. 3, pp. 979–995, Mar. 2012, doi: https://doi.org/10.1016/j.combustflame.2011.10.005.

[36] J. Appel, H. Bockhorn, and M. Frenklach, "Kinetic modeling of soot formation with detailed chemistry and physics: laminar premixed flames of C2 hydrocarbons," *Combustion and Flame*, vol. 121, no. 1–2, pp. 122–136, Apr. 2000, doi: https://doi.org/10.1016/s0010-2180(99)00135-2.

[37] Y. Wang, A. Raj, and S. H. Chung, "A PAH growth mechanism and synergistic effect on PAH formation in counterflow diffusion flames," *Combustion and Flame*, vol. 160, no. 9, pp. 1667–1676, Sep. 2013, doi: https://doi.org/10.1016/j.combustflame.2013.03.013.

[38] "The FORCE: CaltechMech," *Caltech.edu*, 2015. https://www.theforce.caltech.edu/CaltechMech/index.html

[39] M. Frenklach, H. Wang, M. Goldenberg, G. P. Smith, and D. M. Golden, “GRI-MECH: An optimized detailed chemical reaction mechanism for methane combustion. Topical report, September 1992-August 1995,” *Osti.gov*, Nov. 01, 1995. https://www.osti.gov/biblio/200217

[40] University of Southern California, “Welcome to USC Combustion Laboratory,” *Usc.edu*, 2023. https://ignis.usc.edu:80/Mechanisms/USC-Mech%20II/USC_Mech%20II.htm

APPENDICES

Appendix A

Mechanism	Temp at 1%
ABF	1300-1400
Caltech	1300-1400
DLR	1300-1400
KAUST	1300-1400
CRECK	1300-1400
ABF-P	1300-1400

Table A-1: Hydrogen Generation Temperature Comparison at 2-Bar

Mechanism	Temp at 1%
ABF	1300-1400
Caltech	1200-1300
DLR	1200-1300
KAUST	1300-1400
CRECK	1300-1400
ABF-P	1300-1400

Table A-2: Hydrogen Generation Temperature Comparison at 40-Bar

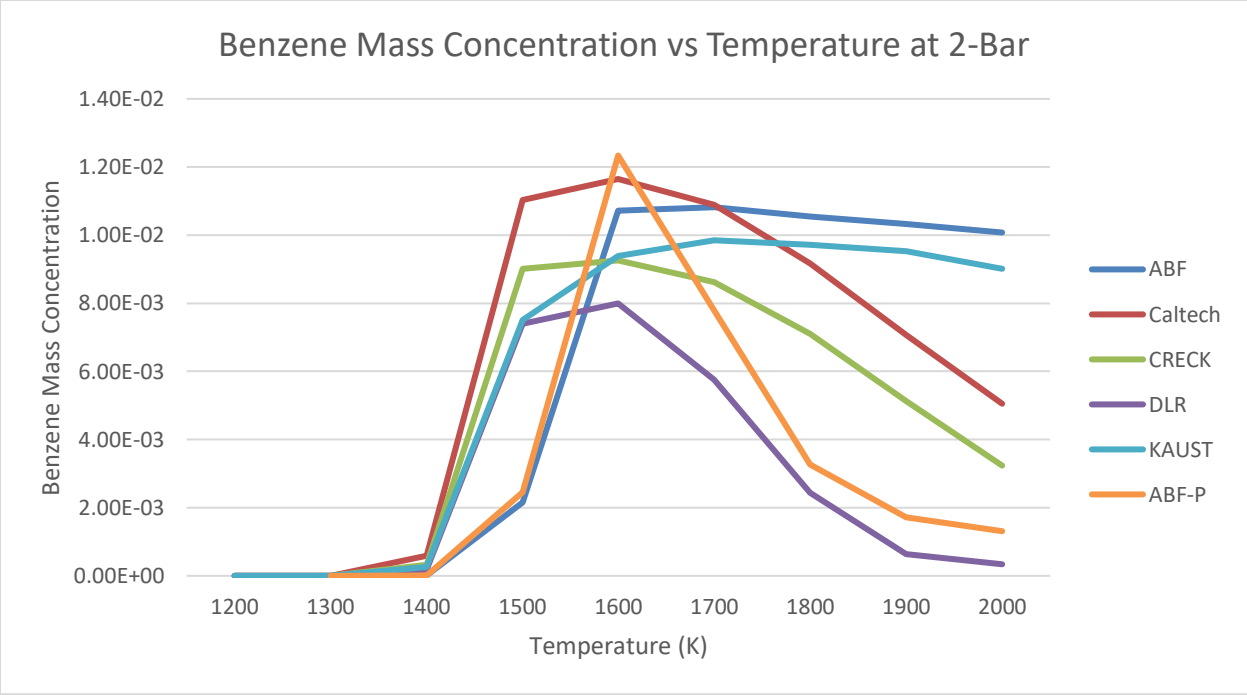

Figure A-1: Benzene Mass Concentration vs Temperature at 2-Bar

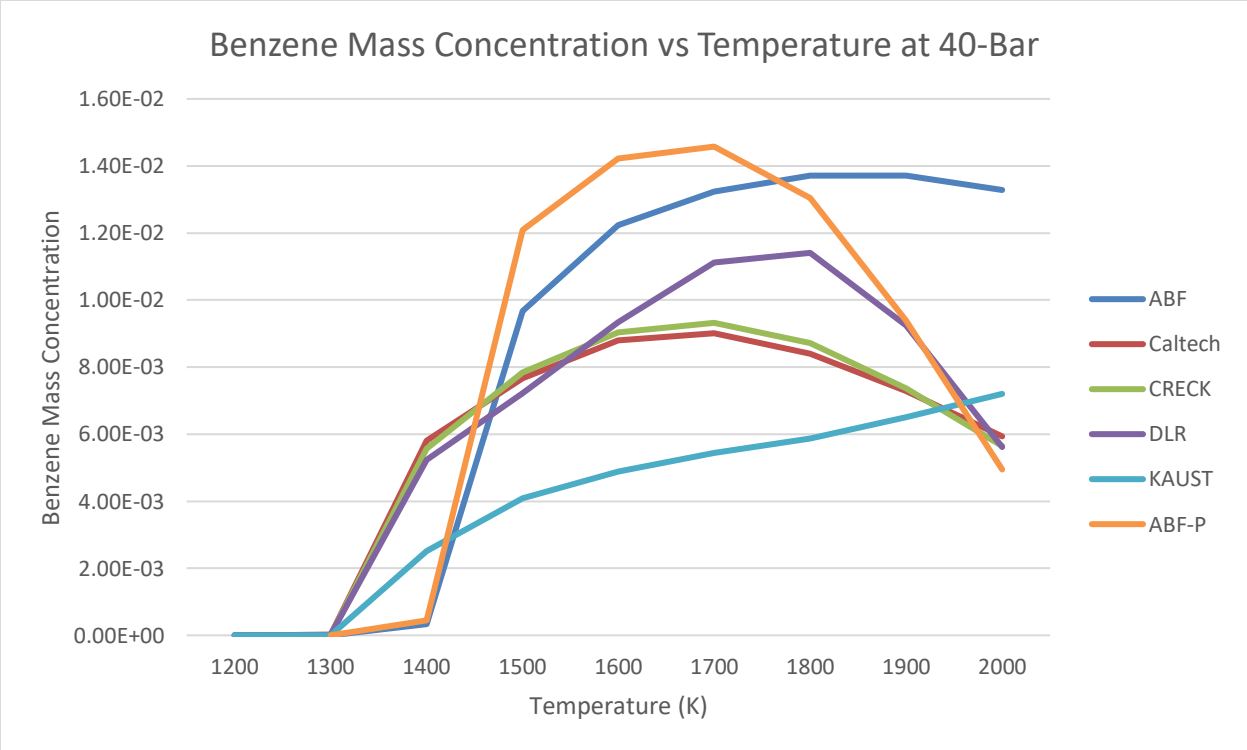

Figure A-2: Benzene Mass Concentration vs Temperature at 40-Bar

VITA AUCTORIS

NAME:	Matthew Veselinovic
PLACE OF BIRTH:	Windsor, ON
YEAR OF BIRTH:	2000
EDUCATION:	St. Thomas of Villanova High School, Windsor, ON, 2018
	University of Windsor, B.Sc., Windsor, ON, 2022
	University of Windsor, M.Sc., Windsor, ON, 2024